CRYSTAL GROWTH & DESIGN

ARTICLE

pubs.acs.org/crystal

Epitaxially Grown Films of Standing and Lying Pentacene Molecules on Cu(110) Surfaces

Tatjana Djuric,*[,†] Thomas Ules,[‡] Heinz-Georg Flesch,[†] Harald Plank,[§] Quan Shen,[∥] Christian Teichert,[∥] Roland Resel,[†] and Michael G. Ramsey[‡]

[†]Institute of Solid States Physics, Graz University of Technology, 8010 Graz, Austria

[‡]Institute of Physics, Karl-Franzens University, 8010 Graz, Austria

[§]Institute for Electron Microscopy, Graz University of Technology, 8010 Graz, Austria

[∥]Institute of Physics, Montanuniversität Leoben, 8700 Leoben, Austria

ABSTRACT: Here, it is shown that pentacene thin films (30 nm) with distinctively different crystallographic structures and molecular orientations can be grown under essentially identical growth conditions in UHV on clean Cu(110) surfaces. By X-ray diffraction, we show that the epitaxially oriented pentacene films crystallize either in the "thin film" phase with standing molecules or in the "single crystal" structure with molecules lying with their long axes parallel to the substrate. The morphology of the samples observed by atomic force microscopy shows an epitaxial alignment of pentacene crystallites, which corroborates the molecular orientation observed by X-ray diffraction pole figures. Low energy electron diffraction measurements reveal that these dissimilar growth behaviors are induced by subtle differences in the monolayer structures formed by slightly different preparation procedures.

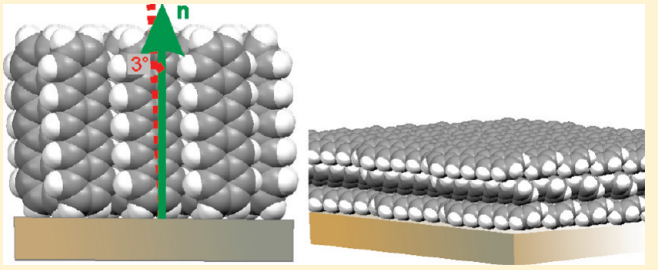

INTRODUCTION

Because of its high charge carrier mobility[1,2] and its ability to form well-ordered films,[3,4] pentacene ($C_{22}H_{14}$), a highly conjugated oligoacene consisting of five benzene rings, has become the material of choice for the active layer in organic thin film transistors. Although pentacene (5A) is already used in commercially available semiconductors, many aspects of its thin film growth are still unclear. Especially, it is remarkable that when deposited in thin films, pentacene crystallizes in various polymorphic phases and molecular orientations. As the crystalline phase and the molecular orientation of the pentacene thin films have a great impact on their electronic properties, understanding the parameters controlling the film structure is important for the development of reliable and reproducible film growth procedures.

To gain a systematical overview of the numerous pentacene (5A) polymorphs reported,[5−12] preferentially, the interplanar spacing of the (001) planes $d_{(001)}$ is used for distinction. The reported bulk phase structures basically can be classified in two different polymorphs: the "bulk" phase with $d_{(001)} \sim 1.45$ nm[5,6] and the "single crystal" phase with $d_{(001)} \sim 1.41$ nm.[6−8] Additionally, thermally evaporated pentacene thin films often exhibit a so-called "thin film" phase with $d_{(001)} \sim 1.54$ nm.[9−11]

Many reasons have been proposed as to why and under which circumstances a specific polymorphic phase and molecular orientation are formed. So far, the substrate material and temperature, the deposition rate, and the final thickness were reported to have a great influence on the crystallographic structure of the pentacene films.[13−17] Especially for the growth of the first monolayer, pentacene molecules tend to grow in an upright orientation when deposited on flat, inert substrates like on SiO_2 or on polymeric dielectrics.[4,13,14,18−21] On reactive surfaces like on clean Si or clean metals, pentacene thin films exhibit an arrangement of flat-lying molecules.[14,22,23] It has been reported that on SiO_2 the substrate temperature and the deposition rate are the parameters determining which polymorphic phase will appear. The "single crystal" phase is favored for high substrate temperatures and low deposition rates. The thin film phase, on the other hand, preferentially grows at low substrate temperatures and high deposition rates.[13] The final thickness of the film was also observed to have an influence on the polymorphic phase: The "thin film" phase dominates at average film thicknesses smaller 50 nm, and above 150 nm, the "single crystal" phase is prevalent.[16] In contrast here with experiments on an atomically clean and controlled Cu(110) substrate surface, we will show that leaving all of the growth parameters constant (substrate, substrate temperature, deposition rate, and film thickness), the different crystallographic structure and the orientation of the films are determined solely by the structure of the first monolayer.

A variety of lying 5A monolayer structures on Cu(110) can be found in the literature;[17,24−28] however, beyond the monolayer, only multilayers with upright molecular orientations have, until now, been

Received: July 16, 2010
Revised: January 15, 2011
Published: March 22, 2011

dx.doi.org/10.1021/cg101230j | *Cryst. Growth Des.* 2011, 11, 1015–1020

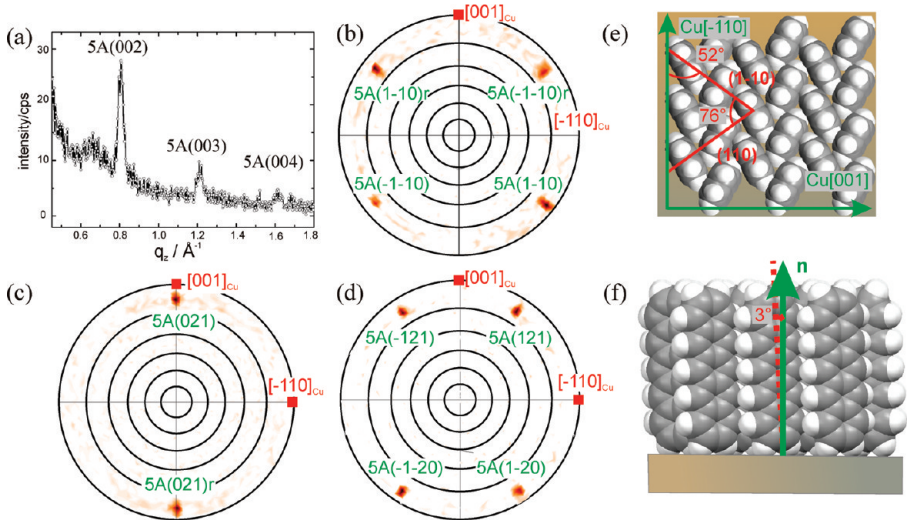

Figure 1. XRD measurements of a pentacene thin film grown on Cu(110). Here, the multilayer was deposited on the monolayer 1. The specular scan reveals that pentacene crystallizes in the "thin film phase" with the (001) net plane parallel to the substrate surface (a). Pole figures measured at $q_z = 1.337$ Å^{-1} (b), $q_z = 1.664$ Å^{-1} (c), and $q_z = 1.989$ Å^{-1} point out that molecules are arranged in epitaxially ordered domains. The top view of this molecular orientation is shown in panel e, and the side view is shown in panel f.

reported.[17,24] From surface energy considerations alone, this might be expected as the (001) net plane (corresponding to upright standing molecules) has a significantly lower energy.[29] However, our previous ultraviolet photoelectron spectroscopy (UPS) studies of 5A film growth on clean Cu(110) have shown that in fact two distinctly different multilayer films with different valence band photoemission signatures and distinct angle-resolved photoemission behavior suggesting films of either upright or lying molecular orientation could be formed.[30,31]

In this work, we investigate the structure of pentacene thin films grown under identical conditions on subtly different monolayers on clean Cu(110) surfaces. The resulting multilayer films are shown to exhibit either the "thin film" phase with standing molecules or the "single crystal" phase with molecules lying with their long molecular axes parallel to the substrate. By studying the evolution of the film structure from the mono- to the multilayer regime, we illuminate the underlying mechanism determining the crystallographic phase and the molecular orientation of the prepared thin films.

EXPERIMENTAL SECTION

The Cu(110) substrate surface was prepared by cleaning the copper crystal by repeated cycles of Ar^+—ion bombardment and annealing to 800 K in a UHV system with a base pressure of 10^{-10} mbar. The pentacene (purchased from Fluka) was deposited in situ from a thoroughly degassed evaporator with a pressure $<10^{-9}$ mbar during the evaporation. The film growth in different stages was monitored in situ by low energy electron diffraction (LEED) and ARUPS measurements. LEED experiments were performed with an Omicron MCP-LEED. Here, a microchannel plate is used to amplify electrons being backscattered by the sample. Because of this amplification, only a low incident beam current in the nA range is needed. Thus, no beam damage or charging problems were encountered even for the relatively thick molecular films.

Generally, when pentacene films are grown directly on the Cu(110) substrate, valence band photoemission and LEED imply that multilayers of upright molecules are formed, while, if such multilayers are thermally desorbed and then a fresh multilayer is grown, it consists of lying molecules. To identify the reason for this different growth behavior, two routes using identical substrate temperatures and deposition rates but resulting in films of either standing or lying molecules were developed. The specific preparation for the upright film characterized here was evaporation of an initial monolayer (4 Å, as monitored by a quartz microbalance assuming a 5A density of 1.33 g cm^{-3}) at room temperature followed by annealing to 180 °C. After cooling down to room temperature on this monolayer (henceforth denoted as monolayer 1), a multilayer was grown at a deposition rate of 5 Å/min to a final thickness of 300 Å. The lying film was prepared by desorbing an upright multilayer film (prepared as above) by annealing it to 180 °C. This leaves a monolayer (denoted as monolayer 2) on which again 300 Å of 5A, at a rate of 5 Å/min, was deposited at room temperature. Note that in both cases the monolayers have been annealed to the same temperature.

The in situ prepared and characterized films were removed from the UHV chamber for the X-ray diffraction (XRD) measurements including specular scans and pole figure measurements. Specular scans determine net planes of the thin film oriented parallel to the substrate by varying the magnitude of the scattering vector in z-direction (perpendicular to the substrate surface). The pole figures are measured by keeping the magnitude of the scattering vector constant while systematically changing its direction. Thereby, the distribution of net plane orientations is obtained, which yields the azimuthal orientation of the pentacene crystallites with respect to the Cu(110) substrate. Specular scans and pole figures were measured with a Philips X'pert X-ray diffractometer using Cr Kα radiation and a secondary side graphite monochromator. The simulation of pole figures was performed with Stereopole,[32] and for the evaluation of the specular scans, Powder Cell[33] was used.

Atomic force microscopy (AFM) measurements of the multilayer films were performed with either a Dimension3100 or a Asylum Research MFP-3D microscope. To minimize lateral forces between tip and surface and consequently to avoid sample damage, tapping mode was used.

RESULTS

Upright Pentacene Films. XRD measurements of a pentacene thin film on Cu(110), where the multilayer was prepared on the monolayer 1, are shown in Figure 1. The specular scan (Figure 1a) reveals that the pentacene film crystallizes in a so-called "thin film" phase ($5A_t$) with the crystallites oriented with the $5A_t(001)$ net plane parallel to the Cu(110) substrate surface. The unit cell parameters as reported by Nabok et al.,[9] $a = 0.592$ nm, $b = 0.754$ nm, $c = 1.563$ nm, $\alpha = 81.5°$, $\beta = 87.2°$, and $\gamma = 89.9°$, imply that the long molecular

dx.doi.org/10.1021/cg101230j |Cryst. Growth Des. 2011, 11, 1015–1020

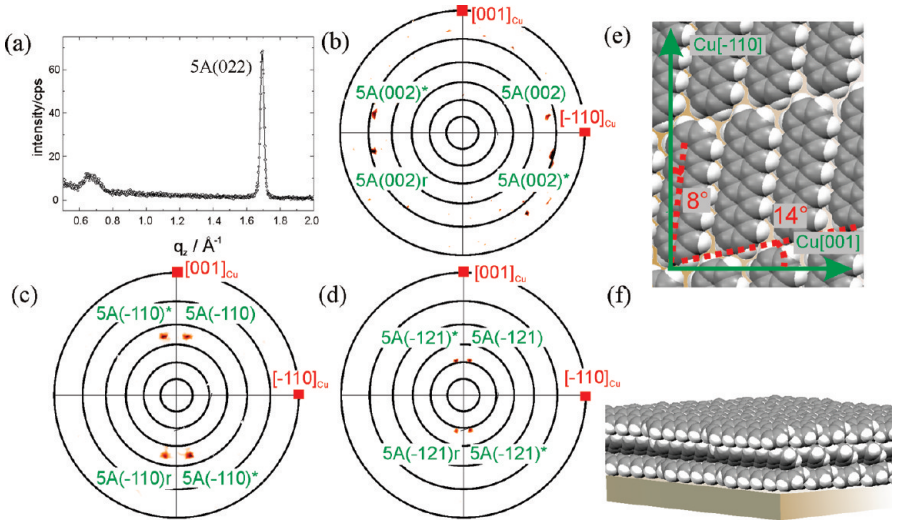

Figure 2. XRD measurements of a pentacene thin film grown on Cu(110) surface. The multilayer film was deposited on the monolayer 2. The specular scan shows that pentacene crystallizes in a "single crystal phase" with the (022) net plane parallel to the Cu(110) substrate surface (a). Pole figures measured at (b) $q_z = 0.89$ Å^{-1}, (c) $q_z = 1.36$ Å^{-1}, and (d) $q_z = 1.99$ Å^{-1} reveal well-ordered, epitaxially aligned domains. The top view of this molecular orientation is shown in panel e, and the side view is shown in panel f.

axes of the molecules are tilted 3° from the surface normal. Pole figure measurements at $q = 1.337$ Å^{-1} (Figure 1b), $q = 1.664$ Å^{-1} (Figure 1c), and $q = 1.989$ Å^{-1} (Figure 1d) corroborate this orientation and furthermore indicate epitaxially well-ordered domains. In the pole figure measured at $q = 1.989$ Å^{-1} (Figure 1d), poles of four different net planes are detected as their q values lie close to each other: (121) $q = 1.976$ Å^{-1}, (1$\bar{2}$0) $q = 1.9861$ Å^{-1}, ($\bar{1}$21) $q = 1.987$ Å^{-1}, and (120) $q = 1.996$ Å^{-1}. The pole figure seen in Figure 1b ($q = 1.337$ Å^{-1}) shows poles of two different net planes having similar q values: (1$\bar{1}$0) $q = 1.351$ Å^{-1} and (110) $q = 1.359$ Å^{-1}. This measurement allows the conclusion that the 5A crystallites are arranged in two domains, which are rotated by 180° to each other, as the two enhanced pole densities (EPDs) belonging to the (1$\bar{1}$0) are higher than those of the (110) plane as theoretically expected. In the case of four equivalent domains, including the mirrored ones, the four EPDs would have a similar magnitude. The azimuthal orientation in the pole figures shows that the pentacene crystallites are aligned with the [031]* crystallographic direction parallel to the [001] azimuth of the copper substrate. The epitaxial alignment deduced from the XRD measurement is illustrated in Figure 1e,f. The top view (Figure 1e) of the (001) net plane shows the characteristic herringbone arrangement. In the side view (Figure 1f), it becomes apparent that the orientation of pentacene molecules is nearly perpendicular to the substrate surface. This molecular orientation is highly advantageous for the charge carrier transport abilities in common transistor geometries, where charge transport parallel to the substrate surface is important. A tilt angle of only ~3° from the substrate surface normal ensures a significant overlap between adjacent π-orbitals.[9,18] Considering the strong tendency of pentacene to form different polymorphic phases when crystallizing in thin films,[13,16,34,35] it is notable that the chosen growth parameters clearly determine one distinct polymorphic phase as the most favorable. For instance, on SiO_2, usually a thin film phase coexists with a single crystal phase, unavoidably leading to grain boundaries, which strongly lower the charge carrier mobility.[36]

The LEED of the multilayer prepared on the monolayer 1 also shows an epitaxially oriented structure but with some rotational disorder. The dimensions of the deduced rectangular unit cell with $a = 0.78$ nm and $b = 0.61$ nm and the unit cell vectors being parallel to the copper azimuths are in perfect accordance with the two-dimensional unit cell of the 5A$_t$(001) net plane found by XRD and thus corroborate standing molecules in the multilayer.

Lying Pentacene Films. In Figure 2, XRD measurements of the film prepared on the monolayer 2 formed by thermal desorption are summarized. Also here, the specular scan (Figure 2a) exhibits only one Bragg peak and thus indicates a single polymorphic phase with one crystal orientation parallel to the substrate surface. The Bragg peak measured at $|q| = 1.69$ Å^{-1} can be assigned to the (022) net plane of a "single crystal" phase [5A$_s$(022)] reported by Mattheus et al.[12] with the following unit cell parameters: $a = 0.6266$ nm, $b = 0.7775$ nm, $c = 1.4530$ nm, $\alpha = 76.475°$, $\beta = 87.682°$, and $\gamma = 84.684°$. This orientation implies that the molecules are lying with their long axes parallel to the surface, while the molecular plane is tilted by ±26° to it. The pole figures measured at $q = 0.89$ Å^{-1} (Figure 2b), $q = 1.36$ Å^{-1} (Figure 2c), and $q = 1.99$ Å^{-1} (Figure 2d) confirm the 5A$_s$(022) net plane as the orientation parallel to the substrate. The EPDs in these pole figures reveal four domains of well-ordered crystallites: domains of crystallites that are rotated by 180° and their mirrored domains. Azimuthally, the crystallites align with the 5A[1$\bar{2}$.10]* [This notation indicates the crystallographic direction, which is parallel to the normal vector of the net plane (1$\bar{2}$.10).] direction parallel to the Cu[$\bar{1}$10] azimuth. For this orientation, the molecules adopt a lying arrangement (see Figure 2e,f) where the long molecular axis encloses an angle of approximately 8 ± 2° with the Cu[$\bar{1}$10] direction .

The LEED measurements of this multilayer film reveal an ordered epitaxially oriented structure. The structure of the multilayer is described by a unit cell with the dimensions $a = 6.2$ Å, $b = 30.3$ Å, and ϕ=79°. This is not the primitive unit cell one would expect from the 2D unit cell of the 5A$_s$(022) net plane measured by XRD ($a = 6.27$ Å, and $b = 14.79$ Å), but it can be explained by a (1×2) reconstruction of the surface of the organic crystallites where, for instance, every second pentacene molecule is either missing or has a different orientation.

dx.doi.org/10.1021/cg101230j |*Cryst. Growth Des.* 2011, 11, 1015–1020

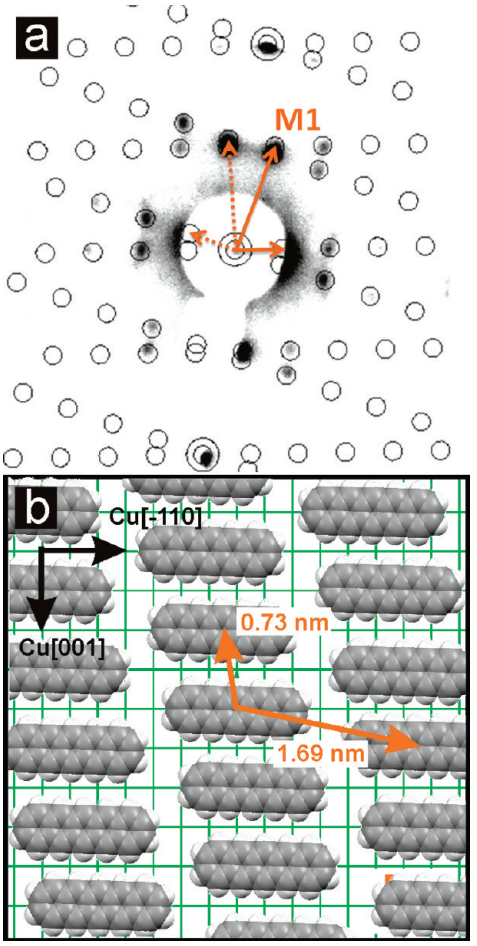

Figure 3. (a) LEED image of the monolayer 1 exhibits one single structure. (b) It is described by an oblique unit cell with parameters: a = 1.69 nm, b = 0.73 nm, and ϕ= 112.9°.

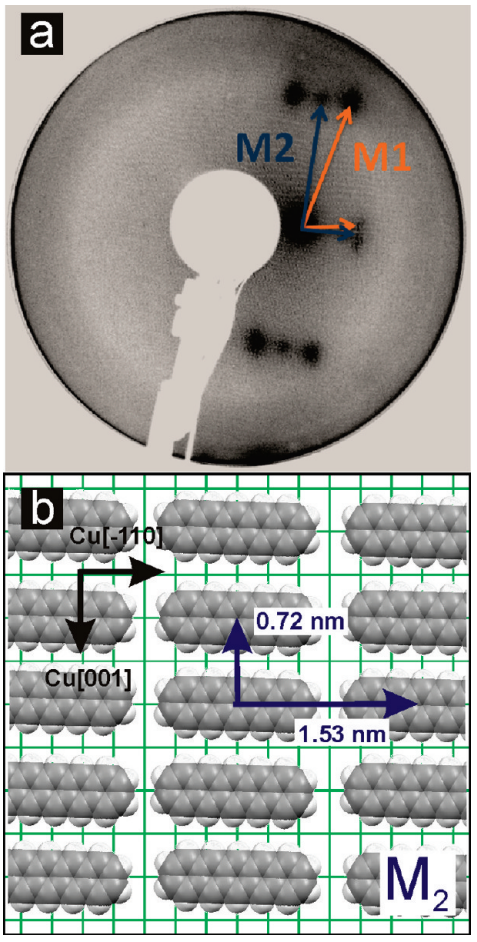

Figure 4. (a) LEED pattern of the monolayer 2 formed by thermal desorption is composed of two different structures. (b) Additionally, to the oblique structure M_1 as observed in the monolayer 1, also a rectangular $p(6 \times 2)$ unit cell is found (M_2).

Monolayer Base for Upright Molecules. For a better understanding of the mechanisms determining the crystallographic structure and the specific epitaxial orientation of the multilayer films, LEED measurements of the first monolayer provide great assistance. The LEED pattern of the monolayer 1 shown in Figure 3a reveals a well-ordered structure. The corresponding oblique unit cell exhibits the parameters a = 1.69 nm, b = 0.73 nm, and ϕ= 112.29° and is described by the following epitaxial matrix

$$M_1 = \begin{pmatrix} 6.5 & -1 \\ -0.5 & 2 \end{pmatrix} \quad (1)$$

which is related to the Cu(110) substrate surface with the unit cell vectors: $a = (2.55, 0)$ and $b = (0, 3.6)$. The epitaxial matrix M_1 indicates a so-called point-online coincidence as both elements in the second column are integers. In this epitaxial alignment, every lattice point of the pentacene monolayer coincides with the $[\bar{1}10]$ line of the Cu(110) substrate. Point-online coincidence is often observed in the organic−inorganic heteroepitaxial growth,[35,37−40] and for these systems, Mannsfeld et al.[41] have demonstrated that such an alignment represents a minimum in the total interface potential. Furthermore, the dimensions of the observed oblique unit cell corroborate an arrangement of flat lying molecules. From UPS measurements, it is known that pentacene adsorbs with its long molecular axis parallel to the Cu(110) substrate and along the Cu$[\bar{1}10]$ crystallographic direction in agreement with (sub)monolayer of the 5A on Cu(110) in the literature.[17,24−28] In the real space image of the monolayer 1, this molecular orientation is used (Figure 3b).

Monolayer Base for the Lying Molecules. The LEED image of the monolayer 2 formed by thermal desorption shows a well-ordered pattern, but only few reflexes are visible (Figure 4a). A detailed analysis reveals that this pattern is composed of two different structures. In addition to the already discussed oblique monolayer structure M_1, also a rectangular unit cell is found, which in the real space can be expressed by the following commensurable epitaxial matrix (see Figure 4b):

$$M_2 = \begin{pmatrix} 6 & 0 \\ 0 & 2 \end{pmatrix} \quad (2)$$

This matrix describes a commensurable, rectangular $p(6 \times 2)$ unit cell with the lattice parameters a = 1.53 nm and b = 0.72 nm. Exactly the same pentacene monolayer structure formed on Cu(110) surfaces was previously reported by Chen et al.[25] A similar $p(6.5 \times 2)$ unit cell was found by Söhnchen et al.[17]

dx.doi.org/10.1021/cg101230j |Cryst. Growth Des. 2011, 11, 1015–1020

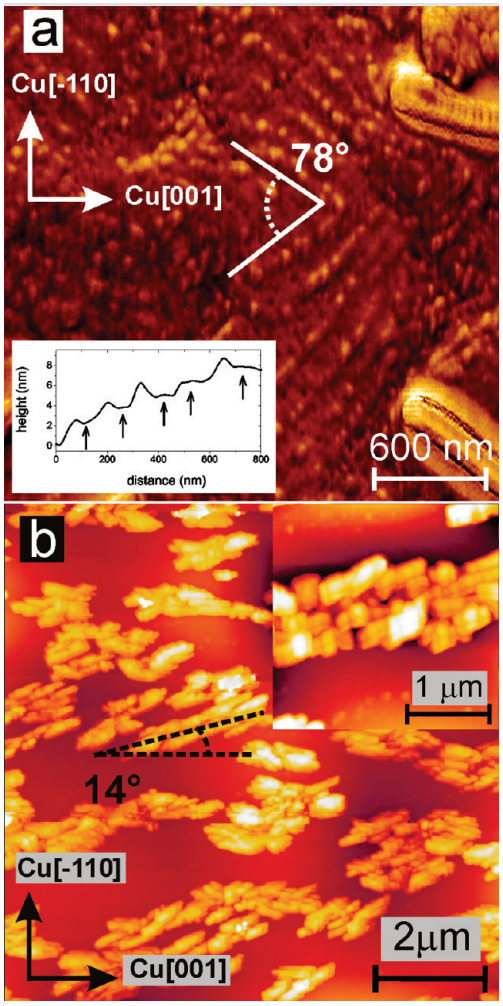

Figure 5. (a) AFM phase scan of the film with standing molecules. The height profile in the inset is taken from a height scan not shown here. (b) 10 μm × 10 μm topography image (color scale: 200 nm), inset: 2.5 μm × 2.5 μm image (color scale: 100 nm). The film consisting of flat-lying molecules exhibits the morphology of elongated islands.

In the LEED patterns of the multilayer, the oblique unit cell (M_1) of the monolayer is still visible, indicating an islandlike growth of the multilayer. Of note is that the rectangular unit cell (M_2) of the monolayer is no longer visible, suggesting that the three-dimensional 5A(022) crystallites grow on these areas, although it cannot be ruled out that the M_2 rearranges. Although both discussed multilayers [$5A_t(001)$, $5A_s(022)$] grow with a defined epitaxial relationship with respect to the monolayers and substrates, their relationship is not simple, and the structures are incommensurable.

Film Morphologies. The AFM images of the film with upright standing molecules [$5A_t(001)$] reveal terraced islands, which are the typical morphology for the growth of upright standing molecules.[15,19,42] The terraces reveal an average step height of 1.4 ± 0.1 nm as expected for upright standing molecules. The scale-up of these terraced islands shows that the terraces form rather distinct angles, suggesting facets of the azimuthally oriented thin film phase crystallites (Figure 5a). The facets as indicated in Figure 5a enclose an angle of approximately 78° around the Cu[001] direction, suggesting the (110) and ($1\bar{1}0$) planes of the crystallites (see Figure 1e). A difference to the standard 5A AFM morphologies reported is that the step edges are decorated with rounded structures of around 50 nm wide and two molecule lengths height. We suggest that these might give rise to the partial rotational disorder observed in LEED. Note, unlike XRD, which showed no evidence for rotational disorder, LEED is surface area sensitive.

The film consisting of 5As(022) crystallites reveals a quite different morphology. Unlike the film of the upright standing molecules [5At(001)], which covers the entire substrate, here, severe islanding is present. Crystallites are covering ~50% of the surface with the wetting monolayer structure M1 between them. The 3D structures consist of crystallites that have aggregated into islands as shown in Figure 5b. These islands are composed of individual grains (see Figure 5b inset) with a typical length of 800 nm, width of 300 nm, and height of 70 nm. Both the angles of the individual crystallites and the agglomerated island and their relation to the underlying Cu azimuth are in accordance to the angles deduced from the XRD measurements (see Figure 2e).

DISCUSSION

Here, we have shown that under identical growth conditions (rate of deposition and substrate temperature), on the same single crystal substrate, two very different epitaxially oriented films of pentacene can be grown. The only identifiable reason for the difference lies in subtle differences in the first monolayers on which the films grow. In the case where the monolayer exhibits an oblique two-dimensional unit cell, the pentacene films grow in an upright fashion in the multilayer [$5A_T(001)$]. However, when the monolayer additionally consists of a rectangular unit cell, the long molecular axes in the multilayer remain parallel to the substrate, while the molecular planes roll by 26° around them, forming the $5A_S(022)$ crystallites. As the monolayers are very similar, in both density and the orientation of the molecules within them, the interaction of adsorbing second layer molecules with the monolayers should be very similar. We therefore speculate that the different crystalline films are a consequence of differences in the kinetics of molecules on the two different wetting monolayer structures. For anisotropic molecules on anisotropic substrates, we have previously shown the importance of one-dimensional diffusion on wetting monolayers for the growth of crystallites of lying molecules.[43] Although the interaction of arriving second layer molecules with the monolayers will be weak, they will orient parallel to the monolayer molecules (i.e., along $[\bar{1}10]_{Cu}$) and will diffuse in this direction. In the case of the rectangular monolayer structure, the one-dimensional diffusion along the monolayer surface corrugation will be undisrupted. Molecules diffusing on neighboring channels can interact and, having their long molecular axes parallel, maximize their interactions, facilitating the formation of critical nuclei of $5A_s(022)$ crystallites, which then grow via sticking to island anisotropy. Such a mechanism has been invoked for the rodlike molecules sexiphenyl and sexithiophene on TiO2(110) and Cu(110)(2 × 1)O substrates, where crystallites of molecules aligned parallel to the substrate surface and surface corrugations are also found.[42,44−46] In contrast, on the oblique monolayer structure (Figure 3b), there are no clear one-dimensional diffusion channels for molecules in the second layer, but rather, zigzag paths will be forced upon them. This will lead to diffusing second layer molecules meeting nonparallel and to become parallel and thus maximize $\pi-\pi$ interactions that they stand up, thus creating seeds for the (001) crystallite orientation. Naturally, this would imply that disordered substrate surfaces will ensure growth of films of upright molecules. Indeed, amorphous substrate surfaces such as Al-oxide, SiO_2, or Si where the first monolayer is strongly bound with a disordered lying monolayer[47] always lead to films of upright molecules. Note that the reactivity of the substrate per se is irrelevant; clean but disordered Cu(110) (sputtered but not annealed) yields a

disordered monolayer of lying molecules on which films of upright pentacene grow.[31] However, unlike on the ordered oblique monolayer, the films are rotationally disordered with no relationship to the substrate azimuths.

CONCLUSION

Epitaxially aligned pentacene multilayer films with two very different types of molecular orientations and polymorphic structures were grown on Cu(110) surfaces. An explanation for the different growth behaviors of the films can be found in subtle differences within the monolayer structures. When the monolayer consists of an oblique unit cell, pentacene molecules grow in epitaxially ordered domains of upright-standing molecules crystallizing in the "thin film" phase with the (001) net plane parallel to the Cu(110) substrate. However, when the monolayer additionally exhibits a rectangular unit cell, molecules arrange with their long molecular axes parallel to the surface and the "single crystal" phase with the (022) net plane parallel to Cu(110) is formed. To be able to fully explain the underlying kinetics driving the specific molecular orientations of these films, further theoretical development of growth dynamics is needed.

ACKNOWLEDGMENT

This work was supported by the Austrian Science Foundation FWF through the national research network: Interface Controlled and Functionalized Organic Films.

REFERENCES

(1) Klauk, H.; Gundlach, D.; Nichols, J.; Jackson, T. *IEEE Trans. Electron Devices* **1999**, *46*, 1258-1263.
(2) Nelson, S. F.; Lin, Y.; Gundlach, D. J.; Jackson, T. N. *Appl. Phys. Lett.* **1998**, *72*, 1854.
(3) Minakata, T.; Imai, H.; Ozaki, M.; Saco, K. *J. Appl. Phys.* **1992**, *72*, 5220.
(4) Laquindanum, J. G.; Katz, H. E.; Lovinger, A. J.; Dodabalapur, A. *Chem. Mater.* **1996**, *8*, 2542–2544.
(5) Campbell, R. B.; Robertson, J. M.; Trotter, J. *Acta Crystallogr.* **1962**, *15*, 289–290.
(6) Siegrist, T.; Besnard, C.; Haas, S.; Schiltz, M.; Pattison, P.; Chernyshov, D.; Batlogg, B.; Kloc, C. *Adv. Mater.* **2007**, *19*, 2079–2082.
(7) Holmes, D.; Kumaraswamy, S.; Matzger, A.; Vollhardt, K. C. *Chem.—Eur. J.* **1999**, *5*, 3399–3412.
(8) Siegrist, T.; Kloc, C.; Schön, J.; Batlogg, B. *Angew. Chem., Int. Ed.* **2001**, *40*, 1732–1736.
(9) Nabok, D.; Puschnig, P.; Ambrosch-Draxl, C.; Werzer, O.; Resel, R.; Smilgies, D. *Phys. Rev. B* **2007**, 76.
(10) Schiefer, S.; Huth, M.; Dobrinevski, A.; Nickel, B. *J. Am. Chem. Soc.* **2007**, *129*, 10316–10317.
(11) Yoshida, H.; Inaba, K.; Sato, N. *Appl. Phys. Lett.* **2007**, *90*, 181930.
(12) Mattheus, C. C.; Dros, A. B.; Baas, J.; Meetsma, A.; Boer, J. L. D.; Palstra, T. T. M. *Acta Crystallogr., Sect. C: Cryst. Struct. Commun.* **2001**, *57*, 939–941.
(13) Dimitrakopoulos, C. D.; Brown, A. R.; Pomp, A. *J. Appl. Phys.* **1996**, *80*, 2501.
(14) Ruiz, R.; Choudhary, D.; Nickel, B.; Toccoli, T.; Chang, K.; Mayer, A. C.; Clancy, P.; Blakely, J. M.; Headrick, R. L.; Iannotta, S.; Malliaras, G. G. *Chem. Mater.* **2004**, *16*, 4497–4508.
(15) Haas, U.; Haase, A.; Maresch, H.; Stadlober, B.; Leising, G. *2004 4th IEEE International Conference on Polymers and Adhesives in Microelectronics and Photonics*, 2004.
(16) Jentzsch, T.; Juepner, H. J.; Brzezinka, K.-W.; Lau, A. *Thin Solid Films* **1998**, *315*, 273–280.
(17) Söhnchen, S.; Lukas, S.; Witte, G. *J. Chem. Phys.* **2004**, *121*, 525.
(18) Mannsfeld, S. C. B.; Virkar, A.; Reese, C.; Toney, M. F.; Bao, Z. *Adv. Mater.* **2009**, *21*, 2294–2298.
(19) Bouchoms, I. P. M.; Schoonveld, W. A.; Vrijmoeth, J.; Klapwijk, T. M. *Synth. Met.* **1999**, *104*, 175–178.
(20) Kalihari, V.; Ellison, D. J.; Haugstad, G.; Frisbie, C. D. *Adv. Mater.* **2009**, *21*, 3092–3098.
(21) Amassian, A.; Pozdin, V. A.; Desai, T. V.; Hong, S.; Woll, A. R.; Ferguson, J. D.; Brock, J. D.; Malliaras, G. G.; Engstrom, J. R. *J. Mater. Chem.* **2009**, *19*, 5580.
(22) Meyer zu Heringdorf, F. J.; Reuter, M. C.; Tromp, R. M. *Nature* **2001**, *412*, 517–520.
(23) France, C. B.; Schroeder, P. G.; Parkinson, B. A. *Nano Lett.* **2002**, *2*, 693–696.
(24) Lukas, S.; Söhnchen, S.; Witte, G.; Wöll, C. *ChemPhysChem* **2004**, *5*, 266–270.
(25) Chen, Q.; McDowall, A. J.; Richardson, N. V. *Langmuir* **2003**, *19*, 10164–10171.
(26) Yamane, H.; Yoshimura, D.; Kawabe, E.; Sumii, R.; Kanai, K.; Ouchi, Y.; Ueno, N.; Seki, K. *Phys. Rev. B* **2007**, *76*, 165436.
(27) Müller, K.; Kara, A.; Kim, T.; Bertschinger, R.; Scheybal, A.; Osterwalder, J.; Jung, T. *Phys. Rev. B* **2009**, *79*, 245421.
(28) Martínez-Blanco, J.; Ruiz-Osés, M.; Joco, V.; Sayago, D. I.; Segovia, P.; Michel, E. G. *J. Vac. Sci. Technol., B* **2009**, *27*, 863.
(29) Nabok, D.; Puschnig, P.; Ambrosch-Draxl, C. *Phys. Rev. B* **2008**, *77*, 245316.
(30) Berkebile, S.; Koller, G.; Fleming, A.; Puschnig, P.; Ambrosch-Draxl, C.; Emtsev, K.; Seyller, T.; Riley, J.; Ramsey, M. *J. Electron Spectrosc. Relat. Phenom.* **2009**, *174*, 22–27.
(31) Ules, T. The initial stages of growth of conjugated molecules; Diploma Thesis, KFU Graz, 2009.
(32) Salzmann, I.; Resel, R. *J. Appl. Crystallogr.* **2004**, *37*, 1029–1033.
(33) Kraus, W.; Nolzeb, G. *J. Appl. Crystallogr.* **1996**, *29*, 301–303.
(34) Oehzelt, M.; Resel, R.; Suess, C.; Friedlein, R.; Salaneck, W. R. *J. Chem. Phys.* **2006**, *124*, 054711.
(35) Koini, M.; Haber, T.; Werzer, O.; Berkebile, S.; Koller, G.; Oehzelt, M.; Ramsey, M.; Resel, R. *Thin Solid Films* **2008**, *517*, 483–487.
(36) Ruiz, R.; Mayer, A. C.; Malliaras, G. G.; Nickel, B.; Scoles, G.; Kazimirov, A.; Kim, H.; Headrick, R. L.; Islam, Z. *Appl. Phys. Lett.* **2004**, *85*, 4926.
(37) Kiyomura, T.; Nemoto, T.; Yoshida, K.; Minari, T.; Kurata, H.; Isoda, S. *Thin Solid Films* **2006**, *515*, 810–813.
(38) Al-Mahboob, A.; Sadowski, J.; Nishihara, T.; Fujikawa, Y.; Xue, Q.; Nakajima, K.; Sakurai, T. *Surf. Sci.* **2007**, *601*, 1304–1310.
(39) Resel, R.; Haber, T.; Lengyel, O.; Sitter, H.; Balzer, F.; Rubahn, H. *Surf. Interface Anal.* **2009**, *41*, 764–770.
(40) Irie, S.; Hoshino, A.; Kuwamoto, K.; Isoda, S.; Miles, M. J.; Kobayashi, T. *Appl. Surf. Sci.* **1997**, *113−114*, 310–315.
(41) Mannsfeld, S.; Fritz, T. *Phys. Rev. B* **2005**, *71*, 056104.
(42) Zhang, F.; Xu, Z.; Liu, X.; Zhao, S.; Lu, L.; Wang, Y.; Xu, X. *Superlattices Microstruct.* **2009**, *45*, 612–617.
(43) Fleming, A. J.; Netzer, F. P.; Ramsey, M. G. *J. Phys.: Condens. Matter* **2009**, *21*, 445003.
(44) Oehzelt, M.; Grill, L.; Berkebile, S.; Koller, G.; Netzer, F. P.; Ramsey, M. G. *ChemPhysChem* **2007**, *8*, 1707–1712.
(45) Al-Shamery, K.; Rubahn, H.; Sitter, H. *Organic Nanostructures for Next Generation Devices*; Springer Berlin Heidelberg: Berlin, Heidelberg, 2008; Bd. 101.
(46) Berkebile, S.; Koller, G.; Hlawacek, G.; Teichert, C.; Netzer, F.; Ramsey, M. *Surf. Sci.* **2006**, *600*, L313–L317.
(47) Kury, P.; Roos, K.; Thien, D.; Möllenbeck, S.; Wall, D.; Horn-von Hoegen, M.; Meyer zu Heringdorf, F. *Org. Electron.* **2008**, 461–465.